

Chemical pressure control of exchange interaction in Mo pyrochlore

Y. Moritomo

CIRSE, Nagoya University, Nagoya 464-8601, Japan

Sh. Xu and A. Machida

Department of Crystalline Materials Science, Nagoya University, Nagoya 464-8603, Japan

T. Katsufuji

Department of Advanced Materials Science, University of Tokyo, Tokyo 113-8656, Japan

E. Nishibori, M. Takata, and M. Sakata

Department of Applied Physics, Nagoya University, Nagoya 464-8603, Japan

S-W. Cheong

Department of Physics and Astronomy, Rutgers University, Piscataway, New Jersey 08854

(Received 30 October 2000; revised manuscript received 8 January 2001; published 22 March 2001)

Structural parameters are systematically investigated for Mo pyrochlore $R_2\text{Mo}_2\text{O}_7$ ($R=\text{Dy}$, Gd , Sm , and Nd) by means of synchrotron radiation x-ray powder diffraction. This system shows a crossover from the spin-glass (SG) state to the ferromagnetic metallic (FM) state as the averaged ionic radius r_R of the rare-earth ion increases. We have found the Mo-O-Mo bond angle increases with r_R from 129.7° for $\text{Dy}_2\text{Mo}_2\text{O}_7$ (SG) to 131.5° for $\text{Nd}_2\text{Mo}_2\text{O}_7$ (FM). This behavior is opposite to the so-called Kanamori-Goodenough rule.

DOI: 10.1103/PhysRevB.63.144425

PACS number(s): 75.50.Cc

I. INTRODUCTION

Recently, pyrochlore compounds $A_2B_2O_7$ attracted great attention because their unusual structure of the corner-sharing tetrahedra can lead to the geometric frustration and interesting low-temperature properties.^{1,2} Due to this geometrical frustration, the spin-glass (SG) phase is expected if the exchange interaction between the neighboring spins is antiferromagnetic. In fact, Dunsiger *et al.*³ have observed the SG phase in $\text{Y}_2\text{Mo}_2\text{O}_7$ and $\text{Tb}_2\text{Mo}_2\text{O}_7$ by means of the muon spin resonance (μSR) measurements and Gardner *et al.*⁴ have observed a glassy-spin state in $\text{Y}_2\text{Mo}_2\text{O}_7$ by the neutron-scattering measurements. In addition to this SG phase, several pyrochlore compounds, e.g., $\text{Y}_2\text{Mn}_2\text{O}_7$ (insulator) and $\text{Tl}_2\text{Mn}_2\text{O}_7$ (metal),⁵ show the ferromagnetic ground state. Recent theoretical investigation⁶ suggests that the frustration arises even when the interaction between the spins are ferromagnetic provided that there exists four local $\langle 111 \rangle$ anisotropy axes.

Another ferromagnetic pyrochlore system is $R_2\text{Mo}_2\text{O}_7$,⁷ where R is a trivalent rare-earth ion: two electrons are accommodated in the t_{2g} orbitals of the Mo $4d$ level. This system undergoes the magnetic transition from the SG insulating state to the ferromagnetic metallic (FM) state as the averaged ionic radius r_R of the rare-earth ion increases.⁷ Taguchi and Tokura⁸ and Katsufuji *et al.*⁹ reported unusual behavior in the ordinary and anomalous Hall coefficients. Recently, Yoshii *et al.*¹⁰ have performed neutron-scattering investigation on a single crystal of $\text{Nd}_2\text{Mo}_2\text{O}_7$ and have revealed that the ferromagnetic transition at $T_C=93$ K is mainly due to the ordering of the Mo spins. The ferromagnetic structure is nearly collinear and the tilting angle θ of the Mo spins from the net magnetization is small. With fur-

ther decrease of temperature below ~ 20 K, ordering of the Nd^{3+} spins takes place.

It is well established that the $M\text{-O-}M$ bond angle (M is a transition metal) governs the magnitude and sign of the superexchange interaction between the neighboring M spins.^{11,12} Actually, Shimakawa *et al.*⁵ have systematically investigated the Mn-O-Mn bond angle θ of the Mn pyrochlore $R_2\text{Mn}_2\text{O}_7$ ($R=\text{In}$, Lu , Tl , and Y) and have found a close interrelation between θ and the Curie temperature T_C . They concluded that the superexchange interaction governs the magnetism of the Mn pyrochlore except for the conducting $\text{Tl}_2\text{Mn}_2\text{O}_7$. Thus, the structural investigation is expected to give us an important clue for understanding of the magnetic interaction of the Mo pyrochlore system.

In this paper, we have systematically investigated structural parameters of the Mo pyrochlores $R_2\text{Mo}_2\text{O}_7$ ($R=\text{Dy}$, Gd , Sm , and Nd) by means of synchrotron radiation x-ray powder diffraction. We have observed systematic variation of the Mo-O-Mo bond angle θ with r_R : θ increases from 129.7° for $\text{Dy}_2\text{Mo}_2\text{O}_7$ ($r_R=1.027$ Å) to 131.5° for $\text{Nd}_2\text{Mo}_2\text{O}_7$ ($r_R=1.109$ Å). This trend is opposite to the so-called Kanamori-Goodenough rule in which the larger bond angle favors the antiferromagnetic-exchange interaction. We have argued the ferromagnetic interaction between the Mo spins in terms of the double-exchange mechanism.

II. EXPERIMENT

A. Sample preparation and characterization

A series of Mo-based pyrochlore $R_2\text{Mo}_2\text{O}_7$ ($R=\text{Dy}$, Gd , Sm , and Nd) was investigated in this work. We have grown crystals of $R=\text{Sm}$ and Nd compounds by the floating-zone

technique. A stoichiometric mixture of commercial Sm_2O_3 , Nd_2O_3 , and MoO_3 was well ground and pressed into a rod with a size of $5 \text{ mm}\phi \times 100 \text{ mm}$ and sintered at 1200°C for 2 h in a flow of Ar gas. The crystal is grown at a feeding speed of $\sim 20 \text{ mm}$ in an Ar atmosphere. Black and shiny crystals typically 4–5 mm in diameter and $\sim 20 \text{ mm}$ in length were obtained. Unfortunately, crystal growth of the small- r_R compound, e.g., $\text{Dy}_2\text{Mo}_2\text{O}_7$ and $\text{Gd}_2\text{Mo}_2\text{O}_7$, is difficult due to the higher melting temperature. We have prepared these compounds by solid-state reaction:⁹ the stoichiometric mixture of R_2O_3 and MoO_3 was reacted in an Ar atmosphere at 1350°C .

Synchrotron radiation x-ray powder-diffraction measurements indicate that all the samples investigated are single phase with cubic ($Fd\bar{3}m; Z=8$) symmetry. We further checked the Mo valence by thermogravimetric analysis and found that the samples are stoichiometric within the resolution of 1% in valence.

B. X-ray structural analysis

In order to get the diffraction patterns with good counting statistics and high angular resolution, synchrotron radiation x-ray powder experiments were carried out at SPring-8 BL02B2. The samples were crushed into fine powder of order of $10 \mu\text{m}$ and were sealed in a $0.2 \text{ mm}\phi$ quartz capillary. Precipitation method was adopted¹³ in order to get a fine powder, which gives a homogeneous intensity distribution in a Debye-Scherrer powder ring. The wavelength of the incident x-ray was $\approx 0.4 \text{ \AA}$ and exposure time was for 5–10 min. We have analyzed thus obtained x-ray powder patterns with RIETAN-97 β program.¹⁴

III. RESULT AND DISCUSSION

A. Magnetization and resistivity

First, let us investigate magnetization and resistivity of the ferromagnetic Mo pyrochlore. Figure 1 shows temperature dependence of (a) magnetization M and (b) resistivity ρ of single crystalline $\text{Sm}_2\text{Mo}_2\text{O}_7$. M was measured under a field of 0.1 T after cooling down to 2 K in the zero field (ZFC) and in the field (FC). For four-probe resistivity measurements, the sample was cut into a rectangular shape typically of $3 \times 2 \times 1 \text{ mm}^3$ and electrical contacts were made with silver paint. With decrease of temperature, the M value steeply increases [see Fig. 1(a)] at $\sim 70 \text{ K}$. The Curie temperature T_C ($=68 \text{ K}$) was determined from the inflection point of the M - T curve. With further decrease of temperature below $\sim 20 \text{ K}$, the magnetization of the ZFC run steeply decreases. A similar behavior is observed also in the ferromagnetic $\text{Nd}_2\text{Mo}_2\text{O}_7$, consistent with Ali *et al.*⁷ This behavior is ascribed to an antiferromagnetic-exchange interaction between R^{3+} and Mo^{4+} spins.^{7,10} As seen in the lower panel [Fig. 1(b)], the ρ - T curve shows metallic behavior in the temperature range investigated ($\leq 300 \text{ K}$). The resistivity curve well scales T^2 ($20 \text{ K} \leq T \leq 50 \text{ K}$) in the ferromagnetic phase perhaps due to the one-magnon-scattering process.¹⁵ Incidentally, the broken curve is the ρ - T curve

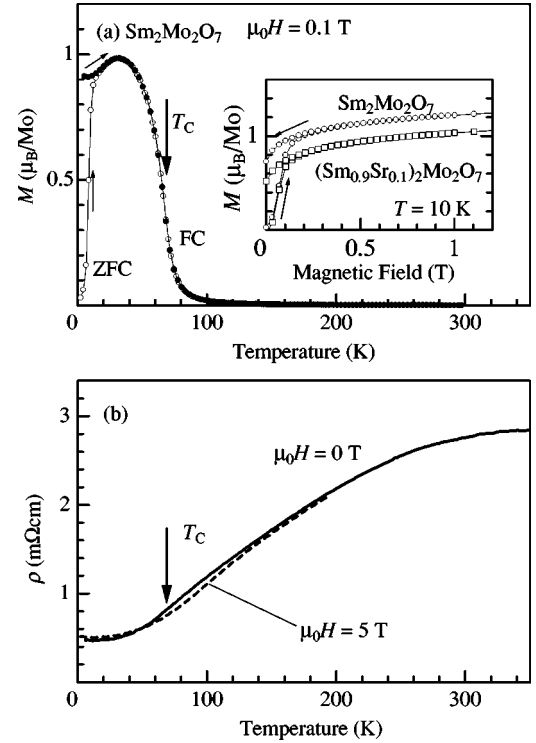


FIG. 1. Temperature dependence of (a) magnetization M and (b) resistivity ρ of single crystalline $\text{Sm}_2\text{Mo}_2\text{O}_7$. M was measured under a field of 0.1 T after cooling down to 2 K in the zero field (ZFC) and in the field (FC). T_C represents the Curie temperature. Inset of the upper panel shows doping effects on the magnetization curve: circles and squares are for $\text{Sm}_2\text{Mo}_2\text{O}_7$ and for $(\text{Sm}_{0.9}\text{Sr}_{0.1})_2\text{Mo}_2\text{O}_7$, respectively. Broken curve in the lower panel is the ρ - T curve measured under a field of 5 T.

measured under a field of 5 T. A large magnetoresistance is observed at around T_C (downward arrow), consistent with the previous work.⁸

The inset of Fig. 1(a) shows doping effects on the magnetization curve: circles and squares are for $\text{Sm}_2\text{Mo}_2\text{O}_7$ and for $(\text{Sm}_{0.9}\text{Sr}_{0.1})_2\text{Mo}_2\text{O}_7$, respectively. The hole-doping procedure into the $\text{Mo}4d$ band significantly suppressed the saturation moment M_s ; M_s decreases from $\approx 1.2\mu_B$ per Mo for $\text{Sm}_2\text{Mo}_2\text{O}_7$ to $\approx 1.0\mu_B$ for $(\text{Sm}_{0.9}\text{Sr}_{0.1})_2\text{Mo}_2\text{O}_7$. In addition, the Curie temperature slightly decreases from $T_C = 68 \text{ K}$ for $\text{Sm}_2\text{Mo}_2\text{O}_7$ to 65 K for $(\text{Sm}_{0.9}\text{Sr}_{0.1})_2\text{Mo}_2\text{O}_7$. These observations suggest that the Mo moment dominates ferromagnetic transition. This is consistent with the neutron scattering experiment:¹⁰ the ferromagnetic transition is mainly due to the ordering of the Mo spins.

Katsufuji *et al.*⁹ have found that the transition temperatures for different combination of R merge into a universal curve against r_R . In the upper panel of Fig. 3, we cited a part of the critical temperatures (squares) for the FM and SG transitions. Open symbols are those for the melt-grown crystals, i.e., $\text{Sm}_2\text{Mo}_2\text{O}_7$ and $\text{Nd}_2\text{Mo}_2\text{O}_7$. With increase of r_R , a crossover behavior from the SG state to the FM state is observed at $\sim 1.047 \text{ \AA}$. This result excludes the possibility that the rare-earth moment governs the exchange interaction between the Mo spins but indicates that the structural parameters are essential for the interaction.

TABLE I. Structural parameters of $R_2\text{Mo}_2\text{O}_7$ ($R = \text{Dy}, \text{Gd}, \text{Sm}, \text{Sm}_{0.9}\text{Sr}_{0.1}$, and Nd) at 300 K determined from synchrotron radiation x-ray diffraction patterns obtained at SPring-8 BL02B2. The crystal symmetry is cubic ($Fd\bar{3}m; Z=8$). The atomic sites are R $16d$ [$\frac{1}{2}, \frac{1}{2}, \frac{1}{2}$], Mo $16c$ [$0, 0, 0$], O1 $48f$ [$u, \frac{1}{8}, \frac{1}{8}$], and O2 $8b$ [$\frac{3}{8}, \frac{3}{8}, \frac{3}{8}$].

Compound	a (Å)	u (Å)	R_{wp} (%)	R_I (%)
$\text{Dy}_2\text{Mo}_2\text{O}_7$	10.2728(1)	0.3331(6)	3.25	4.08
$\text{Gd}_2\text{Mo}_2\text{O}_7$	10.3356(1)	0.3315(8)	4.00	4.05
$\text{Sm}_2\text{Mo}_2\text{O}_7$	10.4196(1)	0.3300(5)	3.29	5.37
$(\text{Sm}_{0.9}\text{Sr}_{0.1})_2\text{Mo}_2\text{O}_7$	10.4781(2)	0.3270(7)	4.26	5.17
$\text{Nd}_2\text{Mo}_2\text{O}_7$	10.4836(2)	0.3297(7)	4.16	7.91

B. Chemical pressure control of structural parameters

Now, let us proceed to the variation of the structural parameters with change of r_R . We summarized in Table I the structural parameters of $R_2\text{Mo}_2\text{O}_7$ derived from the Rietveld analysis of high-angular resolution x-ray powder patterns. In Fig. 2 are shown prototypical examples of the Rietveld refinement at 300 K: (a) $\text{Sm}_2\text{Mo}_2\text{O}_7$ and $\text{Nd}_2\text{Mo}_2\text{O}_7$. The final refinements are satisfactory in which R_{wp} and R_I (reliable factor based on the integrated intensity) are fairly reduced. The insets of both the panels are the magnified patterns (crosses) together with the calculated results (curves). Note that even small Bragg reflections are qualitatively reproduced.

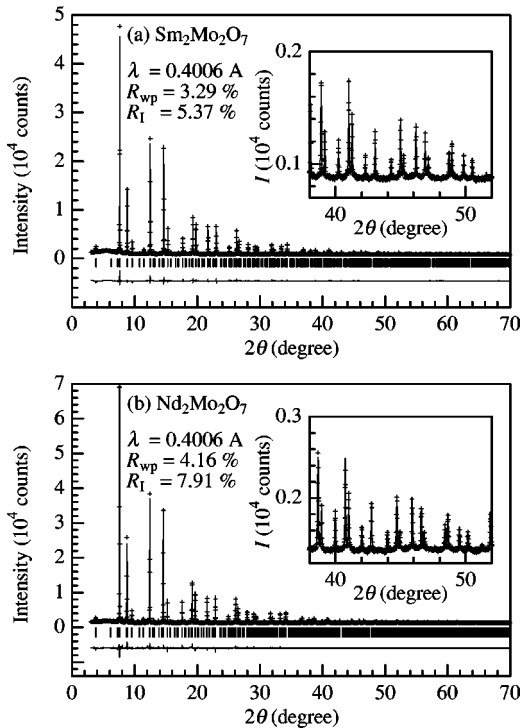


FIG. 2. The whole x-ray powder pattern (crosses) at 300 K for (a) $\text{Sm}_2\text{Mo}_2\text{O}_7$ and (b) $\text{Nd}_2\text{Mo}_2\text{O}_7$. Solid curve is the results of the Rietveld refinement with cubic ($Fm\bar{3}m; Z=8$) symmetry. Insets show the magnified patterns.

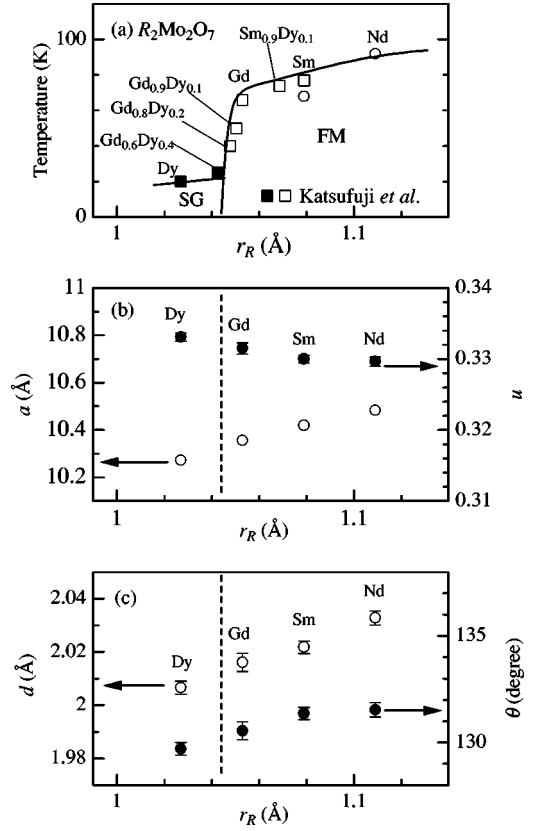


FIG. 3. (a) Critical temperatures for the ferromagnetic (open symbols) and spin-glass (filled symbols) transitions against the averaged ionic radius r_R of rare-earth ion. Data points indicated by squares are cited from Ref. 9. (b) Lattice constant a (open circles) and u parameter (filled circles) of $R_2\text{Mo}_2\text{O}_7$ against r_R . SG and FM represent spin-glass and ferromagnetic metallic phase, respectively. (c) Mo-O bond length d (open circles) and Mo-O-Mo bond angle θ (filled circles) against r_R . Vertical broken lines in (b) and (c) are the SG-FM phase boundary.

In Fig. 3(b) are plotted the lattice parameters of $R_2\text{Mo}_2\text{O}_7$ against r_R together with the magnetic phase diagram [Fig. 3(a); data points indicated by squares are cited from Ref. 9]. How does the structure change as r_R increases? As seen in Fig. 3(b), the u parameter, which specifies the oxygen position ($48f[u, \frac{1}{8}, \frac{1}{8}]$) systematically decreases with r_R . Note that the position of the R (Mo) site is fixed at $16d[\frac{1}{2}, \frac{1}{2}, \frac{1}{2}]$ ($16c[0,0,0]$) in the cubic ($Fd\bar{3}m; Z=8$) symmetry. Based on these structural parameters, we have calculated the Mo-O bond lengths d and the Mo-O-Mo bond angles θ and plotted them in the bottom panel [Fig. 3(c)]. In the lattice structural point of view, increase of r_R causes (1) elongation of d as well as (2) widening of θ .

C. Origin for exchange interaction

Presently observed inter-relation between the exchange interaction and θ , i.e., ferromagnetic-exchange interaction for large θ , is contrary to the Kanamori-Goodenough rule.^{11,12} Here, recall that the ferromagnetic transition is mainly due to the ordering of the Mo spins.¹⁰ According to

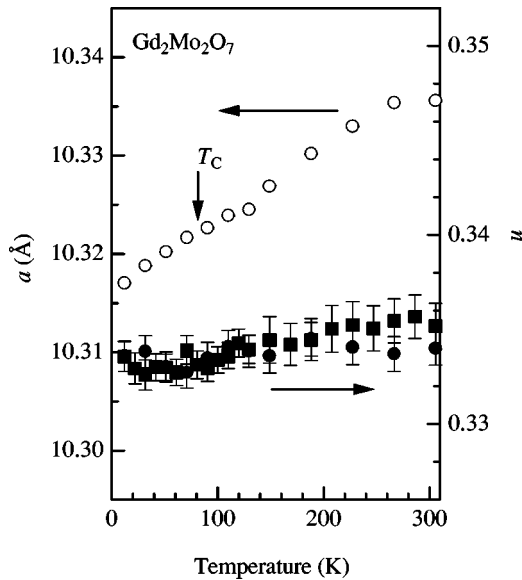


FIG. 4. Temperature variation of lattice constant a (open circles) and u parameter (filled symbols) of $\text{Gd}_2\text{Mo}_2\text{O}_7$. T_C represents the Curie temperature. Circles and squares are determined in the different runs.

this model, the superexchange interaction between the transition metals M via oxygen atoms strongly depends on the M -O- M bond angle. An antiferromagnetic-exchange interaction is expected to occur for a linear bond ($\theta \sim 180^\circ$) while ferromagnetic interaction is often observed for a 90° arrangement.

Another candidate for the origin of the ferromagnetic-exchange interaction is the double-exchange mechanism¹⁶ because the degeneracy of the t_{2g} orbits of the $\text{Mo } 4d$ level can be lifted due to the C_{3h} symmetry of the $[\text{MoO}_6]_7$ cluster. Then, the electrons in the higher-lying level can behave as conducting carriers and mediate the ferromagnetic-exchange interaction between the local Mo spins in the lower-lying level.¹⁷ Within this model, the SG-FM crossover with increase of r_R is ascribed to the suppressed inherent antiferromagnetic-superexchange interaction as well as the enhanced ferromagnetic double-exchange interaction. In addition, the conducting ferromagnetic state (see Fig. 1) and insulating SG state⁹ is consistent with the double-exchange picture.

One may notice that the metallic behavior, i.e., positive temperature differential of resistivity remains even in the high-temperature paramagnetic state. This possibly reflects the fact that the Mo^{4+} (d^2) ion is free from the Jahn-Teller instability. A similar metallic behavior in the paramagnetic state is also observed in the double-exchange ferromagnet $\text{La}_{1-x}\text{Sr}_x\text{MnO}_3$ ($x=0.3-0.4$) (Ref. 18) with the maximal one-electron bandwidth W .¹⁹

D. Temperature variation of structural parameters

Finally, let us investigate the variation of the structural parameters at the magnetic transition. We observed no variation of the Bragg-reflection patterns down to 10 K indicating that the lattice symmetry remains cubic even below T_C . Figure 4 shows the temperature dependence of the lattice constant a (open circles) and the u parameter (filled symbols) of ferromagnetic $\text{Gd}_2\text{Mo}_2\text{O}_7$ ($T_C=66$ K). Surprisingly, no detectable anomaly was observed at T_C (downward arrow) both in a and u . Such a weak coupling between the spin and lattice degrees of freedom is perhaps due to absence of the Jahn-Teller instability.

IV. SUMMARY

In summary, we have systematically investigated structural parameters of the Mo pyrochlores by means of synchrotron radiation x-ray powder diffraction with good counting statistics and high angular resolution. We have observed widening of the Mo-O-Mo bond angle θ as r_R increases. We have discussed the ferromagnetic-exchange interaction between the Mo spins in terms of the double-exchange mechanism. Thus, x-ray powder measurements combined with synchrotron radiation is one of the powerful tools for the investigation of physics of the transition-metal oxides as strongly correlated electron system.

ACKNOWLEDGMENTS

This work was supported by a Grant-in-Aid for Scientific Research from the Ministry of Education, Science, Sports, and Culture. The synchrotron power experiments were performed at the SPring-8 BL02B2 with approval of the Japan Synchrotron Radiation Research Institute (JASRI).

¹M.J. Harris, S.T. Bramwell, D.F. McMorrow, T. Zeiske, and K.W. Godfrey, Phys. Rev. Lett. **79**, 2554 (1997).

²R. Siddharthan, B.S. Shastry, A.P. Ramirez, A. Hayashi, R.J. Cava, and S. Rosenkranz, Phys. Rev. Lett. **83**, 1854 (1999).

³S.R. Dunsiger, R.F. Kiefl, K.H. Chow, B.D. Gaulin, M.J.P. Gingras, J.E. Greedan, A. Keren, K. Kojima, G.M. Luke, W.A. MacFarlane, N.P. Raju, J.E. Sonier, Y.J. Umemura, and W.D. Wu, Phys. Rev. B **54**, 9019 (1996).

⁴J.S. Gardner, B.D. Gaulin, S.H. Lee, C. Broholm, N.P. Raju, and J.E. Greedan, Phys. Rev. Lett. **83**, 211 (1999).

⁵Y. Shimakawa, Y. Kubo, N. Hamada, J.D. Jorgensen, Z. Hu, S.

Short, N. Nohara, and H. Takagi, Phys. Rev. B **59**, 1249 (1999); Y. Shimakawa, Y. Kubo, T. Manako, Y.V. Sushko, D.N. Argyriou, and J.D. Jorgensen, *ibid.* **55**, 6399 (1997).

⁶S.T. Bramwell and M.J. Harris, J. Phys.: Condens. Matter **10**, L215 (1998).

⁷J.E. Greedan, M. Sato, N. Ali, and W. Datars, J. Solid State Chem. **68**, 300 (1987); N. Ali, M.P. Hill, and S. Labroo, *ibid.* **83**, 178 (1989).

⁸Y. Taguchi and Y. Tokura, Phys. Rev. B **60**, 10 280 (1999).

⁹T. Katsufuji, H.Y. Hwang, and S.-W. Cheong, Phys. Rev. Lett. **84**, 1998 (2000).

- ¹⁰S. Yoshii, S. Iikubo, T. Kageyama, K. Oda, Y. Kondo, K. Murata, and M. Sato, J. Phys. Soc. Jpn. **69**, 3777 (2000); Y. Yasui, Y. Kondo, M. Kanada, M. Ito, H. Harashima, M. Sato, and K. Kakurai, *ibid.* **70**, 284 (2001).
- ¹¹J. Kanamori, J. Phys. Chem. Solids **10**, 87 (1958).
- ¹²J.B. Goodenough, Phys. Rev. **100**, 564 (1955).
- ¹³M. Takata, E. Nishibori, K. Kato, M. Sakata, and Y. Moritomo, J. Phys. Soc. Jpn. **68**, 2190 (1999).
- ¹⁴F. Izumi, in *The Rietveld Method*, edited by R.A. Young (Oxford University Press, Oxford, 1993), Chap. 13; Y.-I. Kim and F. Izumi, J. Ceram. Soc. Jpn. **102**, 401 (1994).
- ¹⁵I. Mannari, Prog. Theor. Phys. **22**, 335 (1959).
- ¹⁶P.W. Anderson and H. Hasagawa, Phys. Rev. **100**, 675 (1955).
- ¹⁷In the conducting ferromagnet CrO_2 (Cr^{4+} has two t_{2g} electrons), M.A. Korotin, V.I. Anisimov, D.I. Khomskii, and G.A. Sawatzky, Phys. Rev. Lett. **80**, 4305 (1998) have done the similar argument on the basis of the LAD+ U calculation; The double-exchange-type electronic structure of CrO_2 has been spectroscopically confirmed by R. Yamamoto, Y. Moritomo, and A. Nakamura, Phys. Rev. B **61**, R5062 (2000).
- ¹⁸A. Urushibara, Y. Moritomo, T. Arima, A. Asamitsu, G. Kido, and Y. Tokura, Phys. Rev. B **51**, 14 103 (1995).
- ¹⁹Insulating behavior is observed in the paramagnetic state of narrow- W manganites such as $\text{La}_{1-x}\text{Ca}_x\text{MnO}_3$ due to the strong Jahn-Teller instability or the phase separation instability.